

Disorder-induced melting of the charge order in thin films of $\text{Pr}_{0.5}\text{Ca}_{0.5}\text{MnO}_3$

Z. Q. Yang¹, R. W. A. Hendrikx¹, P. J. M. v. Bentum² and J. Aarts¹

¹ Kamerlingh Onnes Laboratory, Leiden University, P.O. Box 9504, Leiden, the Netherlands

² Nijmegen High Field Magnet Laboratory, Toemooiveld 1, 6525 ED Nijmegen, the Netherlands

PACS. 73.50.Fq { .

PACS. 75.30.Vn { .

March 22, 2024

Abstract. { We have studied the magnetic-field-induced melting of the charge order in thin films of $\text{Pr}_{0.5}\text{Ca}_{0.5}\text{MnO}_3$ (PCMO) films on SrTiO_3 (STO) by X-ray diffraction, magnetization and transport measurement. At small thickness (25 nm) the films are under tensile strain and the low-temperature melting fields are of the order of 20 T or more, comparable to the bulk value. With increasing film thickness the strain relaxes, which leads to a strong decrease of the melting fields. For a film of 150 nm, with in-plane and out-of-plane lattice parameters closer to the bulk value, the melting field has reduced to 4 T at 50 K, with a strong increase in the hysteretic behavior and also an increasing fraction of ferromagnetic material. Strain relaxation by growth on a template of $\text{YBa}_2\text{Cu}_3\text{O}_7$ or by post-annealing yields similar results with an even stronger reduction of the melting field. Apparently, strained films behave bulk-like. Relaxation leads to increasing suppression of the CO state, presumably due to atomic scale disorder produced by the relaxation process.

Introduction. { The occurrence of Charge Order (CO) in doped perovskite manganites of type $\text{RE}_{1-x}\text{A}_x\text{MnO}_3$ (RE = trivalent rare earth, A' = divalent alkaline earth) is currently a much studied phenomenon. The CO state, a long range ordering of the Mn^{3+} and Mn^{4+} ions, is the result of a complicated competition between Coulomb interactions (between the charges), exchange interactions (between the Mn moments), and the electron-lattice coupling. It is therefore sensitive to the amount of doping and to the details of the structure, but also to magnetic fields: the insulating CO state can 'melt' into a metallic state by polarizing the Mn moments and promoting the mobility of the e_g electron on the Mn^{3+} -sites. This magnetic-field-driven insulator-metal transition leads to 'Colossal' magnetoresistance effects [1]. A much studied and quite robust CO-system is $\text{Pr}_{0.5}\text{Ca}_{0.5}\text{MnO}_3$. In the bulk, charge order sets in at 240 K, accompanied by orbital ordering of the e_g -orbitals [2] and an increased distortion of the orthorhombic unit cell [3]. The melting is hysteretic, with field values at low temperatures of about 27 T (increasing field) and 20 T (decreasing field) [4]. In thin film form,

the development and stability of the CO state has been much less studied. A special issue concerns the effects of strain. Given the strong electron-lattice coupling, it can be expected that strained films show properties different from the bulk materials. This is the case, for instance, in tensile strained films of $\text{La}_{0.73}\text{Ca}_{0.27}\text{MnO}_3$ on SrTiO_3 (STO), where very thin (~ 5 nm) films show a Jahn-Teller-like deformed structure, and are insulating rather than metallic [5]. Strain release in thicker films then brings back the bulk properties. Strain should also be present in $\text{Pr}_{0.5}\text{Ca}_{0.5}\text{MnO}_3$ (pseudocubic lattice parameter $a = 0.381$ nm) grown on STO ($a = 0.391$ nm). Recently reported results on this combination demonstrated strongly reduced melting fields [6,7] for films in a thickness range 75 nm – 100 nm, which was ascribed to the fact that the distortions normally induced by the CO state cannot fully develop due to the strain imposed by the substrate.

In the present work, we report on a similar study on $\text{Pr}_{0.5}\text{Ca}_{0.5}\text{MnO}_3$ (PCMO) thin films of varying thickness, deposited on STO-[100] by dc magnetron sputtering, but we come to a different conclusion. At small thickness (25 nm) the strained films still require high CO melting fields H_m of the order of 20 T, quite close to the value of bulk single crystals [4]. With increasing film thickness, the strain relaxes but the bulk-like behavior is increasingly lost; still, in the thickness range around 80 nm, H_m is significantly higher than found in refs [6,7]. At thicknesses around 150 nm the films are almost free of strain and H_m at 50 K has reduced to 4 T, with a strong increase in the hysteretic behavior and the appearance of a ferromagnetic signal. The data suggest that the strain itself does not impede formation of the CO state, but that the relaxation leads to the observed reduction of H_m , presumably due to the generation of lattice defects. This conclusion is supported by the behavior of films which are post-annealed or grown on $\text{YBa}_2\text{Cu}_3\text{O}_7$ (YBCO) as template layer: such films are more relaxed than when grown directly on STO and shows correspondingly smaller values for H_m .

Experimental. { All films studied were sputter deposited from ceramic targets of nominally $\text{Pr}_{0.5}\text{Ca}_{0.5}\text{MnO}_3$ and $\text{YBa}_2\text{Cu}_3\text{O}_7$ on STO substrates, in a pure oxygen atmosphere of 300 Pa with a substrate-source on-axis geometry. The high pressure leads to a very low growth rate of 0.4 nm/min and 2.5 nm/min for PCMO and YBCO respectively. Bilayers were grown by rotating the sample from one target position to the other. The growth temperature was chosen at 840 °C, in order to be able to grow high-quality films of both materials at identical condition. The samples were cooled to room temperature after deposition without post-annealing, which leads to non-superconducting YBCO₇ with $\kappa = 0.53$ (as determined from the lattice parameter). Magnetotransport measurements up to 9 T were performed with an automated measurement platform (called PPM S); magnetization up to 5 T was measured with a SQUID-based magnetometer (both from Quantum Design). Measurements in fields above 9 T were performed in a Bitter magnet at the High Field Magnet Laboratory (Nijmegen). The crystal structure and lattice parameters were characterized by X-ray diffraction, with the lattice parameters out-of-plane determined from the (010)_c, (020)_c and (030)_c reflections (c refers to the pseudocubic cell, with the b-axis taken perpendicular to the substrate), and in-plane from the (013)_c and (023)_c reflections.

Results and discussion. { The structure of bulk PCMO is orthorhombic (Pnma) with $a = 0.5395$ nm, $b = 0.7612$ nm and $c = 0.5403$ nm [8]. In terms of a pseudocubic lattice parameter a_c , this means a slight difference between the a-c plane ($a_c = 0.3818$ nm) and the b-axis ($a_c = 0.3806$ nm). Electron diffraction to determine the film orientation showed that for thin films (below roughly 80 nm) the [010] axis of the film is perpendicular to the substrate, in accordance with the findings of ref. [6]. For thick films (~ 150 nm) the preferential orientation is the same, but domains with the [010]-axis in the substrate plane are also found. The thickness dependence of in-plane and out-of-plane lattice parameters $a_{c,in/out}$ is plotted

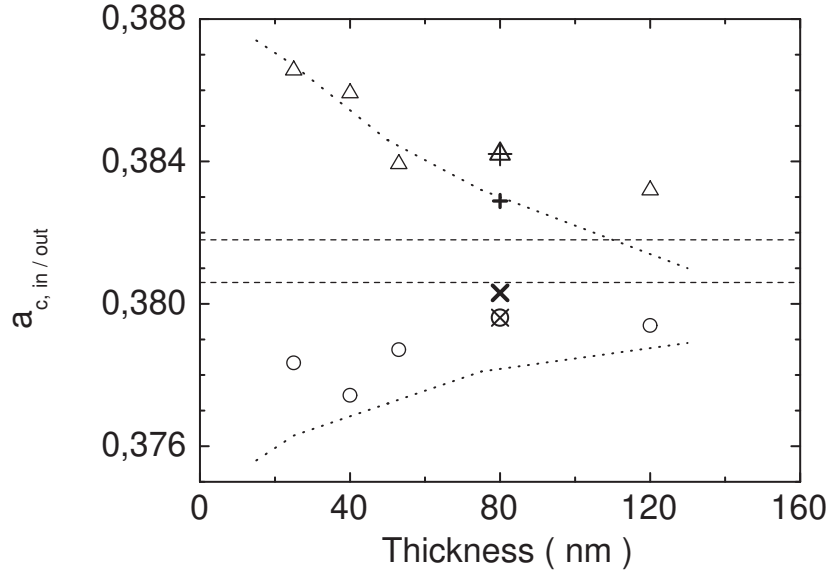


Fig. 1 { Lattice parameters (\circ : out-of-plane $a_{c,out}$; \triangle : in-plane $a_{c,in}$) for films of $\text{Pr}_{0.5}\text{Ca}_{0.5}\text{MnO}_3$ with different thickness. The dotted lines show the behavior for $a_{c,in,out}$ as found in ref. [6]. The horizontal dashed lines indicate the bulk values. The symbols circle/plus and triangle/cross denote a 1-hour post-annealed film of 80 nm; (+, x) denote the same film after a 5-h post-anneal.

in Fig. 1. At low thickness $a_{c,in}$ is closer to the (larger) substrate value than to the bulk value, while $a_{c,out}$ is smaller than the bulk value, indicating that the films grow epitaxially and strained. With increasing thickness both lattice parameters tend towards the bulk values. The behavior is quite similar to that reported in ref. [6] as indicated by the dotted lines in Fig. 1. The full-width-at-half-maximum of the rocking curve of the (020) peak for all films is smaller than 0.5° , indicating good crystallinity.

All films showed semiconductor-like insulating behavior in zero applied magnetic field, as illustrated in Fig. 2a,b for films of 80 nm and 150 nm. An anomaly is present in the logarithmic derivative dR/dT around a value expected for the CO transition temperature T_{CO} , but without the jump which is prominently observed in bulk material at 240 K. The absence of this jump is probably due to the fact that the increase of the in-plane lattice parameter which accompanies the charge ordering is already accommodated by the substrate strain [9]. The CO transition is visible in the magnetization M , especially for the thicker films. As shown in the inset of Fig. 2b, $M(T)$ for the 150 nm film in a field of 1 T shows a clear shoulder around 240 K, reminiscent of the peak in the susceptibility found in the bulk material at T_{CO} (and above the magnetic transition) [10].

For films of 25 nm, the resistance drop in a magnetic field, which signifies the CO melting, was found at temperatures below 100 K near the maximum available field of 20 T for one sample, while a second one did not show a change in R up to 20 T. Also, $R(H)$ is hysteretic: upon decreasing the field the resistance jumps back up at a lower field, as expected since the

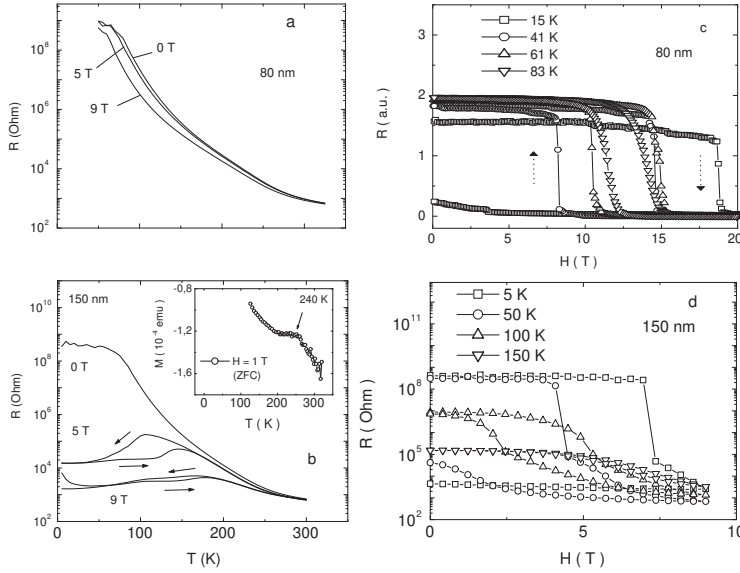


Fig. 2 { Resistance R versus temperature T at magnetic fields $H = 0, 5, 9$ T for films of $\text{Pr}_{0.5}\text{Ca}_{0.5}\text{MnO}_3$ with thickness (a) 80 nm, (b) 150 nm; for the same films R versus H at different T as indicated, (c) 80 nm, (d) 150 nm

melting transition is first order. We denote the upper and lower critical fields as H_c^+ and H_c^- respectively. With increasing thickness, both branches shift to lower fields. Examples of $R(H)$ for the films of 80 nm and 150 nm are given in Fig. 2c,d. For the film of 150 nm the melting field has dropped to only 5 T around 50 K. The resistance changes are sharp, making H_c well-defined, and the curves can be used to construct the temperature-field phase diagrams [11] shown in Fig. 3, where at zero field the value of the bulk is used. The shape of the phase diagrams changes significantly with increasing thickness. For the 25 nm film, hysteresis is only present below 70 K in the field region 16 T – 20 T. These large values resemble the numbers found for bulk single crystals. For the 80 nm film hysteresis starts below 130 K and the difference between the (+; -) branches increase considerably, especially at low temperatures; the H_c^+ branch is still above 12 T at all temperatures, which explains the small MR effects seen in Fig. 2a. Both H_c^+ and H_c^- are considerably larger than reported in ref [7]. In the 150 nm film hysteresis is found below 175 K. Both branches have shifted to lower fields: H_c^+ is curved with a minimum value of 4 T around 50 K, while H_c^- now lies at zero field for temperatures below 80 K.

The melting transition is insulator-metal, but also antiferromagnetic-ferromagnetic, and can therefore be seen in the field dependence of the magnetization. Fig. 4a shows $M(H)$ of the 150 nm film at 100 K, for the field sequence 0 T ! + 5 T ! - 5 T ! + 5 T, with the diamagnetic substrate signal subtracted. A small ferromagnetic component is already present in

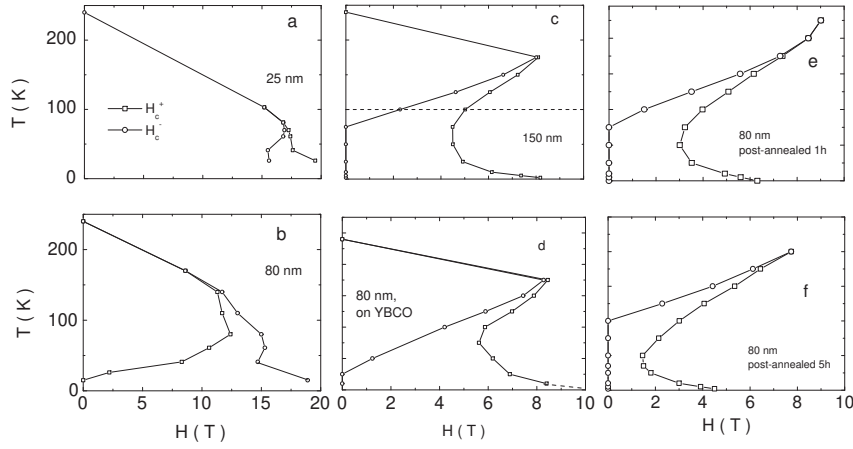


Fig. 3 { Charge order melting field phase diagrams as determined from the magnetoresistance for In s of different thickness. The point at zero field is the bulk value for T_{CO} . (a) 25 nm ; (b) 80 nm ; (c) 150 nm ; (d) 80 nm , grown on YBCO template; (e) 80 nm post-annealed 1h; (f) 80 nm post-annealed 5h. The dashed line in (c) denotes the temperature of the magnetization measurements given in Fig. 4

the virgin state; with increasing field $M(H)$ is constant until 1.8 T and then rises significantly when the field is increased to 5 T. Upon decreasing the field M now remains constant because the sample is in the FM state, but starts to drop around 3 T when H_c is crossed as can be seen in Fig 3c (dotted line). At zero field, the ferromagnetic component has grown by more than a factor 2. The same behavior is found when continuing the loop to -5 T; when going back up to +5 T, M merges with the virgin curve above 4 T.

The first conclusion we draw is that the CO state in the strained material is hardly less stable (if at all) than in the bulk. This is different from the one reached in Refs. [6, 7], but it is in good agreement with the data reported on Cr-doped In s [9]: in that case it was found that strain-free In s very quickly developed ferromagnetism upon Cr-doping, but that Cr-doped In s under tensile strain were still insulating, suggesting that the strain counteracts the effects of the Cr doping and stabilizes the CO state. The decreasing stability of the CO state with increasing In thickness appears due to the strain relaxation rather than the strain itself. The picture arising then is that defects (disorder) induced by the growth and the relaxation destabilize CO, but that the strain itself has no destabilizing effect or even the opposite, which is quite reasonable in view of the fact that the necessary lattice distortion is already accommodated (also suggested in ref. [9]).

In order to highlight the effects of strain relaxation we performed two more experiments. One 80 nm In was annealed in the growth chamber for one hour at 950 °C in 1 mbar O_2 (the sputtering pressure) and slowly cooled; after measuring it was annealed for an additional 5 hours in flowing oxygen at 900 °C. Another 80 nm In was grown on a 10 nm YBCO template layer (called PY) since in previous work [12] we found that YBCO is an effective

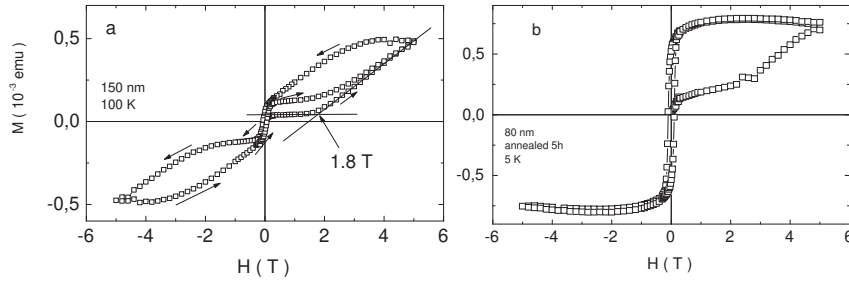


Fig. 4 { Magnetization M versus magnetic field H for thin films of $\text{Pr}_{0.5}\text{Ca}_{0.5}\text{MnO}_3$. In both cases, the magnetization of the substrate has been subtracted. (a) film of 80 nm at 100 K; (b) film of 80 nm, post-annealed for 5h, at 5 K.

strain relaxor for $\text{La}_{0.67}\text{Ca}_{0.33}\text{MnO}_3$. Both methods effectively relax the strain in PCMO as well. Lattice parameter values ($a_{\text{c,out}}$, $a_{\text{c,in}}$) are (0.384 nm, 0.380 nm) for the 1-hour post-annealed sample, (0.383 nm, 0.380 nm) for the 5-hour post-annealed sample, and (0.385 nm, 0.380 nm) for PY, showing that all have undergone relaxation, especially in the out-of-plane axis. The CO-melting phase diagrams for these samples again show a strong decrease of the melting fields (see Fig. 3d-f), with the 5-hour post-annealed sample reaching the lowest value yet observed in this system (1.5 T at about 50 K). The field dependence of the magnetization e.g. at 5 K (Fig. 4b) accordingly shows an increase of M around 3 T (due to the bending back of the H_{C}^+ -branch), but no decrease of M from 5 T downward until the ferromagnetic hysteresis regime is entered, since H_{C} now lies at 0 T.

Since relaxation by post-annealing must be accompanied by inducing defects in the film, the observations reinforce the notion that defects are responsible for the change in melting behavior. In this respect it is important to note that the development of the phase diagrams presented in Fig. 3 closely resembles the changes found in the bulk material when going from $x = 0.5$ (small hysteric regime at a large field) to $x = 0.3$ (curved upper branch at relatively low fields and lower branch going to zero) [1]; especially the similarity between the behavior of the 5h post-annealed film and the $x = 0.3$ bulk material is striking, with both showing a minimum H_{C}^+ field of about 2 T around 30–40 K, and the H_{C} -branch at zero field. Still, the physics behind this may not be quite the same. In the bulk case, the change of doping induces discommensurations and a canted antiferromagnetic (c-a-f) state. In the films the amount of carriers is not changed; rather it is the local structure which can vary, which would influence the local Jahn-Teller distortions and the concomitant orbital order. This would in turn promote ferromagnetic interactions, possibly leading to ferromagnetic clusters in a phase-separation-like scenario very similar to the disorder-driven phase separation observed in films of $\text{La}_{0.67}\text{Ca}_{0.33}\text{MnO}_3$ [13]. We observe that the structure relaxation is accompanied by an increasing amount of ferromagnetic component in the magnetization, which could be either due to the c-a-f state or to ferromagnetic clusters. The answer to this question may come from electron microscopy studies, which are now in progress. Finally, we note that dis-

order as a major source for reduced melting fields can also explain the difference between our results and those of ref. [6,7] as caused by the different morphology of the sputtered versus the laser-ablated films. This suggests that the CO state is more sensitive to disorder than might be assumed in view of the high melting fields, and that if CO films are to be grown, avoiding disorder is the major source of concern.

In summary, we have shown that the melting fields H_m for the insulating CO state in $\text{Pr}_{0.5}\text{Ca}_{0.5}\text{MnO}_3$ films under tensile strain are around 20 T or even above, rather close to the values found for the bulk material. Strain relaxation strongly reduces H_m . With increasing film thickness, the lattice parameters of the film demonstrate relaxation, while H_m decreases down to 4 T at 50 K for a 150-nm film. Upon strain relaxation by post-annealing this value becomes even smaller. We suggest this is due to induced defects, which destabilize the antiferromagnetic state and possibly even promote the formation of ferromagnetic clusters.

This work is part of the research program of the 'Stichting voor Fundamenteel Onderzoek der Materie (FOM)', which is financially supported by NWO.

REFERENCES

- [1] Tokura Y., Tomioka Y., Kuwahara H., Asamitsu A., Moritomo Y. and Kasai M., *Physica C*, 263 (1996) 544
- [2] Kajimoto R., Yoshizawa H., Tomioka Y. and Tokura Y., *Phys. Rev. B*, 63 (2001) 212407
- [3] Damay F., Martin C., Maignan A., Hervieu M. and Raveau B., *Appl. Phys. Lett.*, 73 (1998) 3772
- [4] Tokunaga M., Miura N., Tomioka Y. and Tokura Y., *Phys. Rev. B*, 57 (1998) 5259
- [5] Zandbergen H.W., Freisem S., Nojima T. and Aarts J., *Phys. Rev. B*, 60 (1999) 10259
- [6] Prellier W., Haghiri-Gosnet A.M., Mercey B., Lecoœur Ph., Hervieu M., Simon Ch. and Raveau B., *Appl. Phys. Lett.*, 77 (2000) 1023
- [7] Prellier W., Simon Ch., Haghiri-Gosnet A.M., Mercey B. and Raveau B., *Phys. Rev. B*, 62 (2000) R16337
- [8] Jirak Z., Krupicka S., Simsa Z., Doulka M., and Vratislma S., *J. Magn. Magn. Mater.*, 53 (1985) 153
- [9] Ogimoto Y., Izumi M., Manako T., Kimura T., Tomioka Y., Kawasaki M. and Tokura Y., *Appl. Phys. Lett.*, 78 (2001) 3505
- [10] Jirak Z., Damay F., Hervieu M., Martin, Raveau B., Andre G. and Bouree F., *Phys. Rev. B*, 61 (2000) 1181
- [11] Tomioka Y., Asamitsu A., Kuwahara H., Moritomo Y. and Tokura Y., *Phys. Rev. B*, 53 (1996) R1689
- [12] Yang Z. Q., Hendrikx R. W. A., Aarts J., Qin Y. and Zandbergen H. W., *cond-mat/0102045*,
- [13] Biswas A., Rajeswari M., Srivastava R.C., Li Y.H., Venkatesan T., Greene R.L., and Millis A.J., *Phys. Rev. B*, 61 (2000) 9665